Brief report: Innate lymphoid cells and T-cells contribute to the IL-17A signature detected in the synovial fluid of patients with Juvenile Idiopathic Arthritis

Rosser, Elizabeth; Lom, Hannah; Bending, David; Duurland, Chantal; Bajaj-Elliott, Mona; Wedderburn, Lucy R.

DOI:
10.1002/art.40731

Document Version
Peer reviewed version

Citation for published version (Harvard):
Rosser, E, Lom, H, Bending, D, Duurland, C, Bajaj-Elliott, M & Wedderburn, LR 2018, 'Brief report: Innate lymphoid cells and T-cells contribute to the IL-17A signature detected in the synovial fluid of patients with Juvenile Idiopathic Arthritis', *Arthritis and Rheumatology*. https://doi.org/10.1002/art.40731

Brief Report: Innate lymphoid cells and T-cells contribute to the IL-17A signature detected in the synovial fluid of patients with Juvenile Idiopathic Arthritis

Elizabeth C Rosser PhD[1,2#*], Hannah Lom MSc MRes PhD[1,2*], David Bending PhD[3], Chantal L Duurland MSc PhD[1,4], Mona Bajaj-Elliott PhD[1], Lucy R Wedderburn MD PhD FRCP[1,2,5].

*Authors contributed equally to this work.
[#]Correspondence to e.rosser@ucl.ac.uk

[1]Infection, Immunity, Inflammation Programme, UCL Great Ormond Street Institute of Child Health, London, UK
[2]Arthritis Research UK Centre for Adolescent Rheumatology at UCL, UCLH and GOSH, London, UK
[3]Immunology and Immunotherapy, College of Medical and Dental Sciences, University of Birmingham, Birmingham, UK
[4] Current address: Department of Medical Oncology, Leiden University Medical Center, Leiden, the Netherlands
[5]NIHR Biomedical Research Centre at Great Ormond Street Hospital, London, UK

Abstract

Objective Evidence suggests that aberrant function of innate lymphoid cells (ILC), whose functional and transcriptional profile overlap with T helper (Th) cell subsets, contribute to immune-mediated pathologies. To date, analysis of Juvenile Idiopathic Arthritis (JIA) immune-pathology has concentrated on the contribution of CD4+ T-cells; we have previously identified an expansion of Th17 cells within the synovial fluid (SF) of JIA patients. Here, we extend this analysis to investigate a role for ILC and other IL-17 producing T-cell subsets.

Methods ILC and CD3+ T-cell subsets were defined in peripheral blood mononuclear cells (PBMC) (healthy adult, healthy child and JIA patients) and JIA SF mononuclear cells (SFMC) using flow cytometry. Defined subsets in SFMC were correlated with clinical measures including physician's visual analogue scale (VAS), active joint count and erythrocyte sedimentation rate (ESR). Transcription factor and cytokine profiles of sorted ILC were assessed by qPCR.

Results Group 1 ILC (ILC1), NKp44-group 3 ILC (NCR-ILC3) and NKp44+group 3 ILC (NCR+ILC3) were enriched in the JIA-SFMC compared to PBMC, which corresponded with an increase in transcripts for *TBX21*, *IFNG* and *IL17A*. Of the ILC subsets, NCR-ILC3 frequency in JIA-SFMC displayed the strongest positive association with clinical measures which was mirrored by an expansion in IL-17A+CD4+, IL-17A+CD8+ and IL-17A+$\gamma\delta$ T-cells.

Conclusion We demonstrate that the strength of the IL-17A signature in JIA-SFMC is determined by multiple lymphoid cell-types, including NCR-

ILC3, IL-17A+CD4+, IL-17A+CD8+ and IL-17A+γδ T-cells. These observations may have important implications for the development of stratified therapeutics.

Introduction

Juvenile idiopathic arthritis (JIA), the most common rheumatic disease in childhood, is characterised by joint inflammation lasting longer than 6 weeks [1]. The umbrella term JIA encompasses many subtypes including oligo-articular-JIA (Oligo-JIA), poly-articular-JIA (poly-JIA), enthesitis-related arthritis (ERA), psoriatic-arthritis (PsA) and systemic-JIA [1]. Apart from systemic-JIA, which has a distinct pathogenesis, studies suggest that synovitis in a proportion of JIA cases is linked to IL-23/IL-17A cytokine axis [2]. To date, the IL-17A signature within JIA synovial fluid mononuclear cells (SFMC) has been delineated only in CD4+ T helper (Th) cells.

Emerging evidence indicates that innate lymphoid cells (ILC), the most recently discovered members of the lymphoid family, have critical roles in immunity, tissue development and remodeling [3]. Similarly to Th cells, CD127+ helper ILCs can be divided into distinct groups based upon their functional and transcriptional profile: Th1-equivalent Group 1 ILC (ILC1) express *TBX21* (T-BET) and produce IFNγ, Th2-equivalent group 2 ILC (ILC2) express *GATA3* and produce IL-13, Th17-equivalent natural cytotoxicity receptor (NCR)-group 3 ILC (NCR-ILC3) express *RORC2* and produce IL-17A/IL-22 and Th22-equivalent NCR+ILC3 NCR+ILC3 express *RORC2*, *AHR* and only produce IL-22 [3]. From a clinical viewpoint, chronic ILC activation has been associated with a wide-range of inflammatory disorders [3]. To date, there is no data regarding ILC phenotype/function in childhood arthritides.

Herein, we demonstrate that ILC1, NCR-ILC3, NCR+ILC3 subsets are expanded within JIA-SFMC compared to adult healthy controls, child

healthy controls, and JIA peripheral blood mononuclear cells (PBMC) but that NCR-ILC3 show the strongest association with multiple measures of clinical severity. Notably, the increase in NCR-ILC3 within JIA-SFMC was accompanied with an increase in IL-17 producing CD4+, CD8+ and $\gamma\delta$ T-cells. These data suggest that the IL-17 signature previously observed in JIA-SFMC CD4+ T-cells may extend to the ILC compartment and other T-cell subsets.

Patients and methods

Human Samples

Peripheral blood (PB) from healthy adult (aHC), child controls (cHC) and JIA patients, and synovial fluid (SF) from JIA patients were obtained with fully informed and age-appropriate consent as approved by the London-Bloomsbury Research Ethics Committee (ref: 95RU04) in accordance with the Declaration of Helsinki. Clinical subtypes of JIA were defined according to International League of Associations for Rheumatology criteria (ILAR) [1]. Clinical and demographical data are shown in Supplementary Table 1. PB and SF mononuclear cells (PBMC and SFMC) were prepared by density gradient centrifugation. Before processing, SF samples were treated with Hyaluronidase (10U/ml; Sigma-Aldrich) for 30 mins at 37°C.

Flow Cytometry, Image Stream and Cell Sorting

Flow cytometry was performed using directly conjugated monoclonal antibodies (listed in Supplementary Table 2) as described [2]. Dead cells were excluded using a live/dead discrimination dye (Thermo Scientific). ILC were defined as cells within the lymphocyte gate that were single cells, lineage negative (CD1a, CD3, CD11c, CD14, CD16, CD19, CD34, CD94, CD123, BDCA2, FcεRIα, αβTCR and γδTCR), CD45+, CD127+ and CD161+. ILC subpopulations were defined according to phenotype: ILC1 (CRTH2-cKit-) ILC2 (CRTH2+) NCR-ILC3 (CRTH2-cKit+NKp44-) and NCR+ILC3 (CRTH2-cKit+NKp44+) [4]. Data were acquired on LSRII flow cytometer (BD) and analysed using FlowJo software version 10.1

(TreeStar Inc.). For Image stream analysis, ILC were stained and analysed on Amnis ImagestreamX Mark II (Merck Millipore). For cell sorting, ILC were stained as above and sorted on a FACSAriaIII (BD).

RNA extraction and qRT-PCR

RNA was routinely extracted from sorted (~50,000-100,000) ILCs using the Arcturus Picopure RNA isolation kit (ThermoFisher Scientific) and cDNA synthesized (iScript DNA kit;Bio-rad) according to manufacturer's instructions. cDNA was amplified using SYBR Green Mastermix (Bio-rad) with custom primers for *AHR, RORC2, GATA3, TBX21, IL17A, IL22, IL13* and *IFNG* (Life Technologies); primer sequences are listed in Supplementary Table 3. For each sample, transcript quantity was normalized to β–actin (*ACTB*) expression.

Statistical analysis

Statistical analysis was performed using Prism 5.03 (Graphpad). In bar charts data represent standard error of the mean. For comparison of two groups Mann-Whitney U Tests were used. For multiple comparison testing, Kruskal-Wallis tests with Dunn's multiple comparison tests were performed. P values of less than 0.05 were considered significant and indicated on graphs. Spearman's correlation with Bonferroni's correction for multiple testing was used for correlation analyses, uncorrected p values and the adjusted Bonferroni alpha cut-off are reported in Supplementary Table 4.

Results

Expansion of ILC1, NCR-ILC3 and NCR+ILC3 in JIA-SFMC.

ILC (lineage-CD45+CD127+CD161+), were enumerated within PBMC and SFMC of JIA patients and PBMC of adult (aHC) and child (cHC) healthy controls (Figure 1A and B). The ILC population was small as a proportion of all live mononuclear cells in both compartments (0.005-0.5% of total live mononuclear cells) consistent with other reports in human adult PBMC [4]. There were no significant differences in the proportion of ILC within all mononuclear cell populations tested (Figure 1A and B).

Next, we determined whether there were differences in ILC subsets, as a proportion of total ILC, in PBMC *versus* SFMC. ILC subsets were identified as ILC1 (CRTH2-cKit-); ILC2 (CRTH2+); and ILC3 (CRTH2-cKit+), which were divided into NCR+ and NCR- subgroups according to expression of NKp44. Given the low frequency of ILC populations, ImageStream analysis was used to confirm that both PBMC and SFMC ILC subtypes were lymphoid in morphology and that antibody staining was localized to the membrane prior to analysis (Supplementary Fig. 1A). Assessment of ILC subset frequency showed that ILC1 cells were significantly enriched as a proportion of total ILC in JIA-SFMC compared to JIA-PBMC, aHC and cHC-PBMC (Figure 1C and D). Further analyses revealed that the largest differences in ILC1 frequency was observed between PBMC and SFMC from patients with oligo-JIA (Figure 1D) complementing historic data demonstrating that T-cells from oligo-JIA patients produce a significant amount of IFNγ [5]. ILC2, which have been implicated in the resolution of chronic joint inflammation by supporting

Treg function [6], were significantly lower in SFMC compared to PBMC from patients or controls, with both oligo-JIA and ERA displaying a significant difference between SFMC and aHC-PBMC (Figure 1C and E). These differences may reflect the larger number of ERA-JIA and oligo-JIA patients analysed in our cohort.

Within the ILC3 compartment, the proportion of NCR-ILC3 was significantly higher in SFMC compared to aHC-PBMC or JIA-PBMC and this effect was observed in all JIA subtypes (Figure C and 1F). There was a significant enrichment of NCR+ILC3, which were present at very low frequency in PBMC from patients and controls, in SFMC from all JIA subtypes compared to aHC (Figure 1C, F and G). No differences were observed in the frequency of ILC subsets amongst PBMC or SFMC between all JIA subtypes analysed.

Transcriptional profile of ILC within JIA-SFMC is altered compared to ILC within PBMC

Increasing evidence indicates that ILC1, ILC2, NCR-ILC3 and NCR+ILC3 express specific transcription factors and cytokine profiles that parallel Th1, Th2, Th17, Th22 cells respectively [3, 4]. Accordingly, we next assessed whether variation in the frequency of ILC subsets observed in PBMC *versus* SFMC was associated with an altered transcriptional profile. Gene expression analysis of transcription factors (*TBX21, GATA3, RORC2, AHR*) and cytokines (*IFNG, IL13, IL17A, IL22*) by qPCR in SFMC ILC relative to aHC-PBMC ILC demonstrated that there was a significant

increase in type-1 associated *TBX21* and *IFNG* and a significant decrease in type-2 associated *GATA3* and *IL13* mirroring the changes in subset frequency we had observed by flow cytometry (Figure 2A and B). Analysis of transcription factors and cytokines associated with ILC3 subsets demonstrated a significant increase in the relative expression of *IL17* and a trend for an increase in *RORC2, AHR* and *IL22* although the expression varied between JIA-SFMC samples (Figure C and D). Due to the small amount of blood taken from children we were unable to isolate sufficient ILC from cHC or JIA-PBMC to perform qPCR analysis.

Changes in ILC subset frequency within the synovial fluid of patients with JIA are associated with disease severity

As the ILC subset frequency and transcriptional profile was altered in JIA-SFMC, we next investigated whether these changes were associated with clinical measure of disease severity. Physician's visual analogue scale (VAS), active joint count, and erythrocyte sedimentation rate (ESR) were correlated with the proportion of ILC1, NCR+ILC3 or NCR-ILC3 within total ILC within SFMCs. ILC2 were not included in these analyses due their paucity within SFMC. This exploratory analysis showed promising trends that the frequency of ILC1, NCR+ILC3 and NCR-ILC3 subsets were associated with disease severity (Figure 2E and Supplementary Table 4). Notably, whilst ILC1 and NCR-ILC3 positively associated with an increase in physician's VAS, there was a negative correlation between physician's VAS and NCR+ILC3. One potential hypothesis is that NCR+ILC3 may also

be important in the resolution of joint inflammation in JIA, similarly to observations previously reported in the inflamed gastrointestinal tract in ankylosing spondylitis [7]. Potential correlation between ILC subset frequency and active joint count or ESR was next assessed. A positive association between NCR-ILC3 cells and active joint count and a weak association between NCR-ILC3 and ESR was observed (Figure 2F-G and Supplementary Table 4). No association between ILC1 and NCR+ILC3 and active joint count or ESR was seen. Markedly, no differences in the frequency of SFMC ILC1, NCR-ILC3 and NCR+ILC3 were observed between treatment-naïve *versus* patients on methotrexate (Supplementary Figure 1B-D).

Expansion of NCR-ILC3 in synovial fluid of JIA patients is associated with an increase in IL-17A producing CD4+ T-cells, CD8+ T-cell and γδ T-cells

Herein, we have demonstrated that ILC subset frequency, transcriptional profile is altered in SFMC isolated from JIA and that of the ILC subsets identified within the JIA-SFMC an expansion of NCR-ILC3 has the strongest association with multiple measures of clinical severity. NCR-ILC3 can be characterized by the expression of RORC and IL-17A, similarly to Th17 cells, and can be found expanded in IL-17A driven pathologies [8]. Taken together, these data suggest that the IL-17A CD4+ T-cell signature we have previously described in JIA SF may extend to other cell-types including ILC [2]. To investigate this, we quantified other

potential IL-17A producing cell types; this included CD4+ T-cells, CD8+ T-cells, γδ T-cells. As previously described [2], we found higher percentages of IL-17A+CD4+ cells within JIA-SFMC compared to healthy and JIA-PBMC (Figure 3A). Analysis of IL-17A+CD8+ and IL-17A+CD4-CD8- (of which ~80% were γδ T-cells, data not shown) cells established that there was also a significantly higher percentage of IL-17A+CD8+ and a trend for an increase in IL-17A+CD4-CD8- in JIA-SFMC compared to aHC-PBMC and JIA-PBMC (Figure 3B and C). No significant differences were seen between aHC, cHC and JIA-PBMC. Unlike the enrichment of NCR-ILC3 within the SFMC of all subtypes of JIA (Figure 1F), there were significant differences in the frequency of IL-17A-producing T-cells between JIA subtypes. For example, in agreement with published reports demonstrating a strong IL-17A signature in ERA, we found an increase in IL-17A-producing CD4+, CD8+ and CD4-CD8- T-cells in SFMCs isolated from ERA patients (Figure 3A-C) [9]. It is worth highlighting however that there was a proportion of patients that displayed a strong IL17A signature regardless of subtype.

To assess whether the IL-17A T-cell-signature was associated with an expansion of NCR-ILC3, a correlation analysis was performed between the various synovial subpopulations analysed. Positive correlations were observed in SFMC between NCR-ILC3 as a proportion of total live cells and IL-17A-positive cells in the CD4+ and CD8+ T-cell compartments (Figure 3D and E and Supplementary Figure 4). A weak potential association with IL-17A+CD4-CD8- T-cells was also observed (Figure 3F and Supplementary Figure 4). These data demonstrate that the expansion

of NCR-ILC3 is concomitant with the expansion of IL-17A producing T-cells within JIA-SFMC; indicating that the cell specific contribution to the IL-17A milieu in JIA-SFMC may be a key determinant of clinical outcome. Of note, correlation between the percentage of IL-17+CD4+, IL-17+CD8+ and IL-17+CD4-CD8 with physician's VAS, active joint count and ESR demonstrated that of the T-cell subsets, CD4+ T-cells had the strongest association with physicians VAS (Supplementary Figure 2 and Supplementary Figure 4). However unlike NCR-ILC3, the percentage of IL-17A+ T-cell subsets did not have any association with active joint count or ESR.

DISCUSSION

Recent investigation into ILC biology and function has led to an appreciation of their role in tissue/immune homeostasis and their contribution to immunopathology. However, this is the first study to investigate whether ILC phenotype and function is altered in JIA. We demonstrate that ILC1, NCR-ILC3 and NCR+ILC3 are expanded within JIA-SFMCs. Most interestingly, NCR-ILC3, the innate equivalent to Th17 cells [10], exhibit a positive association with disease severity and with an increase in multiple IL-17A producing T-cell subsets. Future studies are needed to confirm our hypothesis that the strength of the IL-17A signature within JIA SFMC is shared amongst multiple cell-types.

Both human studies and animal models support a central role for IL-17A in JIA pathogenesis. For example, IL-17A-deficient mice are resistant to the induction of collagen-induced arthritis (CIA) [11] and levels of IL-17A are known to be significantly higher in the JIA SF [9]. However, the relative contribution of different cell-types to IL-17A production within the inflamed joint remains relatively unexplored. Our data show that both innate, namely NCR-ILC3, and adaptive lymphoid cells, namely T-cells (CD4+, CD8+ and $\gamma\delta$), may contribute to IL-17A production at the inflammatory site. Further work is needed to unravel the mechanisms that underlie the preferential accumulation of multiple IL-17A-producing cell-types with JIA-SFMC. One possible explanation is that the presence of high levels of IL-1β, IL-23 and IL-6 within the synovial environment of JIA [12] creates an “IL-17A-skewing” micro-environment that induces the

differentiation of Th17 cells and ILC3 [3, 13]. Future studies using single cell RNA sequencing will aid in defining detailed functional and transcriptional heterogeneity in SFMC-ILC as recently reported for human tonsils [14]. At present our data demonstrate the presence of an inflammatory type-1 and type-17 transcriptional signature in total SFMC-ILC but not which ILC1/ILC3 subset is responsible for this transcriptional signature. This is especially pertinent as it is not yet known how the inflammatory environment of the arthritic joint alters the plasticity of ILC1/ILC3 subsets.

Despite success of JIA treatment with TNFα- and IL-6-blockade, a group of patients remain unresponsive to treatment. Here, our exploratory analysis demonstrate that disease severity could potentially be associated with an increase in multiple IL-17 producing lymphoid cell-types. This suggests that IL-17A targeting treatments could be efficacious in a significant proportion of JIA patients (who may fall into several of the current clinically defined subtypes). This notion is further supported by recent evidence showing that Secukinumab, a monoclonal antibody against IL-17A, is effective in the treatment of ankylosing spondylitis, another IL-17A-driven autoimmune disease [15]. Our observations raise the possibility that patients may be better stratified for treatment with biologics based on immune-phenotype rather than by previously ascribed clinical categories. It is now essential to gain a whole-system view of IL-17A biology in order to design novel therapeutic strategies.

Acknowledgements

We would like to thank Dr P. Blair for comments on the manuscript and Dr C Deakin for her statistical expertise. This work is funded by a PhD studentship for H. Lom awarded to LR Wedderburn through the Arthritis Research UK and GOSCC funded Centre for Adolescent Rheumatology at UCL GOSH and UCLH (20164); Arthritis Research UK Foundation fellowship awarded to EC Rosser by (21141); Arthritis Research UK Foundation fellowship awarded to D Bending (19761); 7th Framework programme of the EU, SP3-People, support for training and career development for researchers (Marie Curie), Network for Initial Training (ITN), FP7-PEOPLE-2011-ITN, under the Marie Skłodowska-Curie grant agreement No. 289903 to CL Duurland; SPARKS UK to CL Duurland and LR Wedderburn (08ICH09 and 12ICH08). This research was supported by the NIHR Great Ormond Street Hospital Biomedical Research Centre. The views expressed are those of the author(s) and not necessarily those of the NHS, the NIHR or the Department of Health.

Author Contributions

All authors were involved in drafting the article or revising it critical for important intellectual content, and all authors approved the submitted manuscript. LR Wedderburn and EC Rosser had full access to all of the data in the study and take responsibility for the integrity of the data and the accuracy of the data analysis.

Study conception and design. Rosser, Lom, Bending and Wedderburn.

Acquisition of data. Rosser, Lom and Duurland.

Analysis and interpretation of data. Rosser, Lom, Bending, Duurland, Bajaj-Elliott, Wedderburn.

References

1. Petty RE, Southwood TR, Manners P, Baum J, Glass DN, Goldenberg J, He X, Maldonado-Cocco J, Orozco-Alcala J, Prieur AM *et al*: **International League of Associations for Rheumatology classification of juvenile idiopathic arthritis: second revision, Edmonton, 2001**. *J Rheumatol* 2004, **31**(2):390-392.
2. Nistala K, Moncrieffe H, Newton KR, Varsani H, Hunter P, Wedderburn LR: **Interleukin-17-producing T cells are enriched in the joints of children with arthritis, but have a reciprocal relationship to regulatory T cell numbers**. *Arthritis Rheum* 2008, **58**(3):875-887.
3. Artis D, Spits H: **The biology of innate lymphoid cells**. *Nature* 2015, **517**(7534):293-301.
4. Hazenberg MD, Spits H: **Human innate lymphoid cells**. *Blood* 2014, **124**(5):700-709.
5. Gattorno M, Facchetti P, Ghiotto F, Vignola S, Buoncompagni A, Prigione I, Picco P, Pistoia V: **Synovial fluid T cell clones from oligoarticular juvenile arthritis patients display a prevalent Th1/Th0-type pattern of cytokine secretion irrespective of immunophenotype**. *Clin Exp Immunol* 1997, **109**(1):4-11.
6. Rauber S, Luber M, Weber S, Maul L, Soare A, Wohlfahrt T, Lin NY, Dietel K, Bozec A, Herrmann M *et al*: **Resolution of inflammation by interleukin-9-producing type 2 innate lymphoid cells**. *Nat Med* 2017, **23**(8):938-944.
7. Ciccia F, Accardo-Palumbo A, Alessandro R, Rizzo A, Principe S, Peralta S, Raiata F, Giardina A, De Leo G, Triolo G: **Interleukin-22 and interleukin-22-producing NKp44+ natural killer cells in subclinical gut inflammation in ankylosing spondylitis**. *Arthritis Rheum* 2012, **64**(6):1869-1878.
8. Leijten EF, van Kempen TS, Boes M, Michels-van Amelsfort JM, Hijnen D, Hartgring SA, van Roon JA, Wenink MH, Radstake TR: **Brief report: enrichment of activated group 3 innate lymphoid cells in psoriatic arthritis synovial fluid**. *Arthritis Rheumatol* 2015, **67**(10):2673-2678.

9. Agarwal S, Misra R, Aggarwal A: **Interleukin 17 levels are increased in juvenile idiopathic arthritis synovial fluid and induce synovial fibroblasts to produce proinflammatory cytokines and matrix metalloproteinases**. *J Rheumatol* 2008, **35**(3):515-519.
10. Kiss EA, Diefenbach A: **Role of the Aryl Hydrocarbon Receptor in Controlling Maintenance and Functional Programs of RORgammat(+) Innate Lymphoid Cells and Intraepithelial Lymphocytes**. *Front Immunol* 2012, **3**:124.
11. Nakae S, Nambu A, Sudo K, Iwakura Y: **Suppression of immune induction of collagen-induced arthritis in IL-17-deficient mice**. *J Immunol* 2003, **171**(11):6173-6177.
12. de Jager W, Hoppenreijs EP, Wulffraat NM, Wedderburn LR, Kuis W, Prakken BJ: **Blood and synovial fluid cytokine signatures in patients with juvenile idiopathic arthritis: a cross-sectional study**. *Ann Rheum Dis* 2007, **66**(5):589-598.
13. Lee Y, Awasthi A, Yosef N, Quintana FJ, Xiao S, Peters A, Wu C, Kleinewietfeld M, Kunder S, Hafler DA *et al*: **Induction and molecular signature of pathogenic TH17 cells**. *Nat Immunol* 2012, **13**(10):991-999.
14. Bjorklund AK, Forkel M, Picelli S, Konya V, Theorell J, Friberg D, Sandberg R, Mjosberg J: **The heterogeneity of human CD127(+) innate lymphoid cells revealed by single-cell RNA sequencing**. *Nat Immunol* 2016, **17**(4):451-460.
15. Baeten D, Sieper J, Braun J, Baraliakos X, Dougados M, Emery P, Deodhar A, Porter B, Martin R, Andersson M *et al*: **Secukinumab, an Interleukin-17A Inhibitor, in Ankylosing Spondylitis**. *N Engl J Med* 2015, **373**(26):2534-2548.

Figure Legends

Figure 1. ILC1, NCR-ILC3 and NCR+ILC3 are expanded in the SF of patients with JIA. (A) Representative flow cytometry plots and (B) summary scatter plots with bar charts showing the frequency of total ILC (defined as Lineage-CD127+CD161+) within total CD45+ live cells in adult healthy (aHC, n=12) PBMC, child healthy (cHC, n=4) PBMC, JIA-PBMC (total n=15, ERA n=8, oligo-JIA n=4, poly-JIA n=2, PsA n=3) and JIA-SFMC (total n=38, ERA n=17, oligo-JIA n=13, poly-JIA n=3, PsA n=5). (C) Representative flow cytometry plots and (D-G) summary scatter plots with bar charts showing the frequency of (D) ILC1 (defined as Lineage-CD127+CD161+cKit-CRTH2-), (E) ILC2 (defined as Lineage-CD127+CD161+CRTH2+), (F) NCR-ILC3 (defined as Lineage-CD127+CD161+cKit+CRTH2-NKp44-) and (G) NCR+ILC3 (defined as Lineage-CD127+CD161+cKit+CRTH2-NKp44+) within total ILC in adult healthy (aHC, n=12) PBMC, child healthy (cHC, n=4) PBMC, JIA-PBMC (total n=15, ERA n=8, oligo-JIA n=4, poly-JIA n=2, PsA n=3) and JIA-SFMC (total n=38, ERA n=17, oligo-JIA n=13, poly-JIA n=3, PsA n=5). Statistical analysis carried out by Kruskal Wallis with Dunn's multiple comparison tests. Bar charts represent mean ± SE.

Figure 2. Changes in ILC subset frequency within total SFMC ILCs is associated with changes in transcriptional profile in and clinical severity. Summary scatter plots with bar charts showing the relative expression of (A) *TBX21* and *IFNG*, (B) *GATA3* and *IL13*, (C) *RORC2* and *IL17A*, (D) *AHR* and *IL22* in SFMC (n=5) versus PBMC (n=5) as measured by qPCR. Statistical analysis carried out by Mann-Whitney U Tests. Bar charts represent mean ± SE. (E-G) Scatter plots showing relationship between (E) physician's VAS (n=24), (F) active joints (n=27), (G) ESR (n=18) and the frequency of ILC1, NCR-ILC3 and NCR+ILC3 within total live cells in JIA-SFMC at time of sample. Statistical analysis carried out by

Spearman correlation analysis with Bonferroni's correction for multiple testing.

Figure 3. IL-17A-producing CD4+, CD8+ and γδ T-cells in JIA SF. (A-C) Representative flow cytometry plots and summary scatter plots with bar charts showing the frequency of IL-17A+ cells within (A) CD4+ cells, (B) CD8+ T-cells and CD4-CD8- in CD3+ gated live cells in aHC-PBMC (n=12), child healthy cHC (n=6) PBMC, JIA-PBMC (total n=25, ERA n=13, oligo-JIA n=4, poly-JIA n=6, PsA n=3) and JIA-SFMC (total n=41, ERA n=17, oligo-JIA n=8, poly-JIA n=6, PsA n=10). Statistical analysis carried out by Kruskal Wallis with Dunn's multiple comparison tests. Bar charts represent mean ± SE. (D-F) Scatter plots showing relationship between the frequency of (D) IL-17A+CD4+ T-cells, (E) IL-17A+CD8+ T-cells and (F) IL-17A+CD4-CD8- T- cells with percentage of NCR-ILC3 within total live cells in JIA-SFMC (n=16). Statistical analysis carried out by Spearman correlation analysis with Bonferroni's correction for multiple testing.

Supplementary Figure 1. SFMC-ILC subsets have the same morphology as PBMC-ILC subsets and their frequency are not altered by treatment status. ILC subsets were identified according to fluorescence of subset specific protein expression by analysis of individual cell images as shown using image stream. Representative images of ILC subsets from (A) PBMC and (B) SFMC from JIA patients. All ILC detected had a characteristically dense single nuclei, a thin halo of perinuclear cytoplasm, were approx 7μm and had cell markers restricted to the cell surface. Left hand panel (grey) shows the brightfield image. Summary scatter plots with bar charts showing the frequency of (C) ILC1, (B) NCR-ILC3 and (E) NCR+ILC3 with JIA-SFMC of treatment naïve JIA patients 9n=14) and patients on methotrexate (n=17). Bar charts represent mean ± SE.

Supplementary Figure 2. IL-17A+ T cell subsets can be associated with clinical measure of disease severity. Scatter plots showing relationship between (A) physician's VAS (n=15), (B) active joints (n=21) and (C) ESR (n=17) and the frequency of IL-17+CD4+ T cells, IL-

17+CD8+ T cells and IL-17+CD4-CD8- T cells within JIA-SFMC. Statistical analysis carried out by Spearman correlation analysis with Bonferroni's correction for multiple testing.

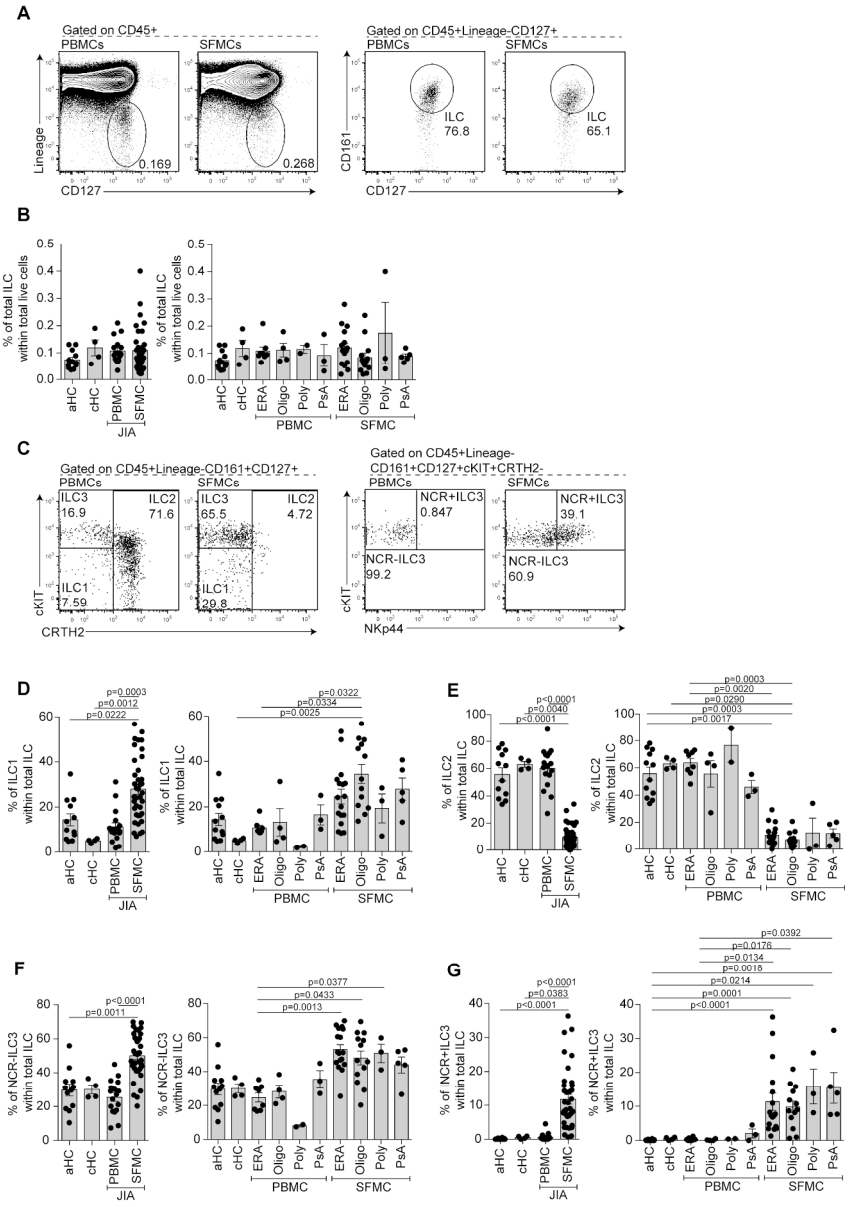

FIGURE 1: ILC1, NCR-ILC3 and NCR+ILC3 are expanded in the SF of patients with JIA. (A) Representative flow cytometry plots and (B) summary scatter plots with bar charts showing the frequency of total ILC (defined as Lineage-CD127+CD161+) within total CD45+ live cells in adult healthy (aHC, n=12) PBMC, child healthy (cHC, n=4) PBMC, JIA-PBMC (total n=15, ERA n=8 oligo-JIA n=4, poly-JIA n=2, PsA n=3) and JIA-SFMC (total n=38, ERA n=17 oligo-JIA n=13, poly-JIA n=3, PsA n=5). (C) Representative flow cytometry plots and (D-G) summary scatter plots with bar charts showing the frequency of (D) ILC1 (defined as Lineage-CD127+CD161+cKit-CRTH2-), (E) ILC2 (defined as Lineage-CD127+CD161+CRTH2+), (F) NCR-ILC3 (defined as Lineage-CD127+CD161+cKit+CRTH2-NKp44-) and (G) NCR+ILC3 (defined as Lineage-CD127+CD161+cKit+CRTH2-NKp44+) within total ILC in adult healthy (aHC, n=12) PBMC, child healthy (cHC, n=4) PBMC, JIA-PBMC (total n=15, ERA n=8 oligo-JIA n=4, poly-JIA n=2, PsA n=3) and JIA-SFMC (total n=38, ERA n=17 oligo-JIA n=13, poly-JIA n=3, PsA n=5). Statistical analysis carried out by Kruskal Wallis with Dunn's multiple comparison tests. Bar charts represent mean ± SE.

188x268mm (300 x 300 DPI)

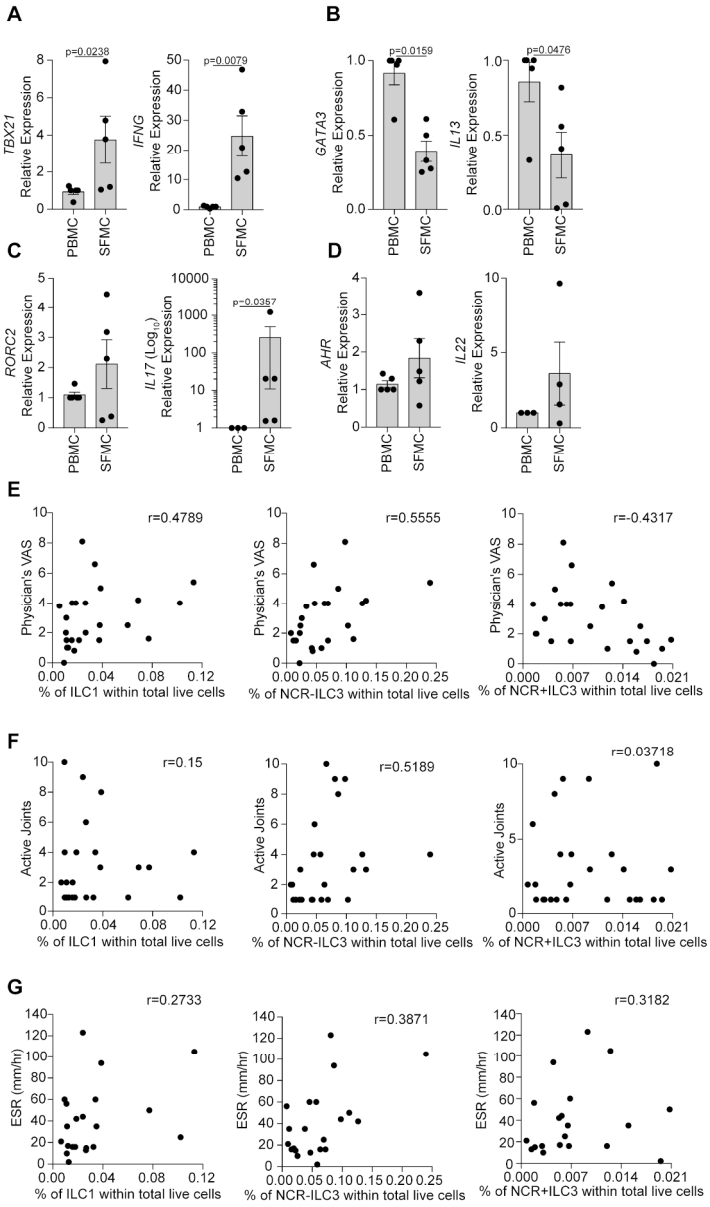

FIGURE 2: Changes in ILC subset frequency within total SFMC ILCs is associated with changes in transcriptional profile in and clinical severity. Summary scatter plots with bar charts showing the relative expression of (A) TBX21 and IFNG, (B) GATA-3 and IL-13, (C) RORC2 and IL-17A, (D) AhR and IL-22 in SFMC (n=5) versus PBMC (n=5) as measured by qPCR. Statistical analysis carried out by Mann-Whitney U Tests. Bar charts represent mean ± SE. (E-G) Scatter plots showing relationship between (E) physician's VAS (n=24), (F) active joints (n=27), (G) ESR (n=18) and the frequency of ILC1, NCR-ILC3 and NCR+ILC3 within total live cells in JIA-SFMC at time of sample. Statistical analysis carried out by Spearman correlation analysis with Bonferroni's correction for multiple testing.

143x244mm (300 x 300 DPI)

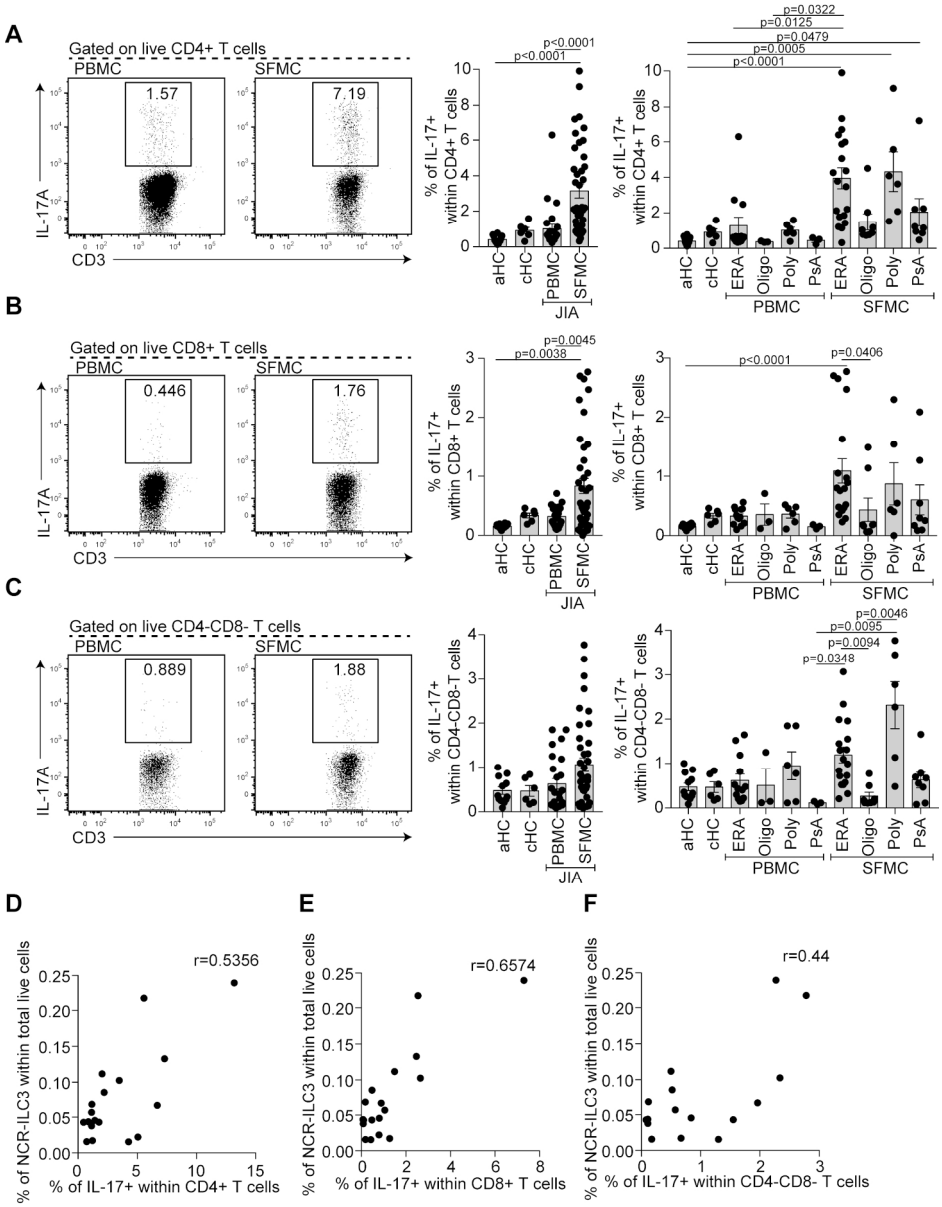

FIGURE 3: IL-17A-producing CD4+, CD8+ and γδ T-cells in JIA SF. (A-C) Representative flow cytometry plots and summary scatter plots with bar charts showing the frequency of IL-17A+ cells within (A) CD4+ cells, (B) CD8+ T-cells and CD4-CD8- in CD3+ gated live cells in aHC-PBMC (n=12), child healthy cHC (n=6) PBMC, JIA-PBMC (total n=25, ERA n=13, oligo-JIA n=4, poly-JIA n=6, PsA n=3) and JIA-SFMC (total n=41, ERA n=17, oligo-JIA n=8, poly-JIA n=6, PsA n=10). Statistical analysis carried out by Kruskal Wallis with Dunn's multiple comparison tests. Bar charts represent mean ± SE. (D-F) Scatter plots showing relationship between the frequency of (D) IL-17A+CD4+ T-cells, (E) IL-17A+CD8+ T-cells and (F) IL-17A+CD4-CD8- T- cells with percentage of NCR-ILC3 within total live cells in JIA-SFMC (n=16). Statistical analysis carried out by Spearman correlation analysis with Bonferroni's correction for multiple testing.

159x205mm (300 x 300 DPI)

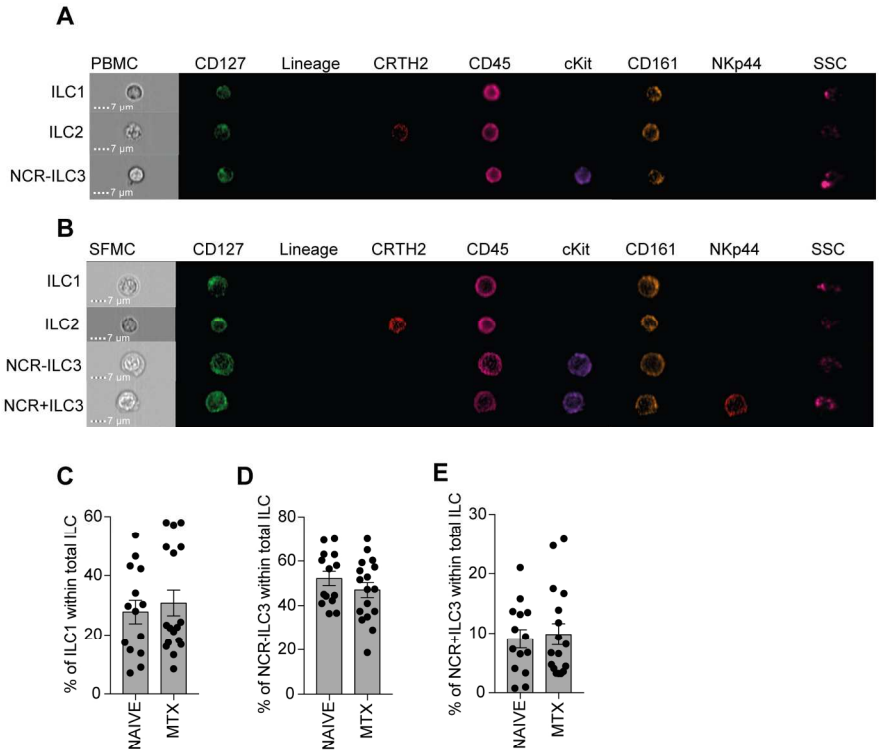

SUPPLEMENTARY FIGURE 1: SFMC-ILC subsets have the same morphology as PBMC-ILC subsets and their frequency are not altered by treatment status. ILC subsets were identified according to fluorescence of subset specific protein expression by analysis of individual cell images as shown using image stream. Representative images of ILC subsets from (A) PBMC and (B) SFMC from JIA patients. All ILC detected had a characteristically dense single nuclei, a thin halo of perinuclear cytoplasm, were approx 7µm and had cell markers restricted to the cell surface. Left hand panel (grey) shows the brightfield image. Summary scatter plots with bar charts showing the frequency of (C) ILC1, (B) NCR-ILC3 and (E) NCR+ILC3 with JIA-SFMC of treatment naïve JIA patients 9n=14) and patients on methotrexate (n=17). Bar charts represent mean ± SE.

171x180mm (300 x 300 DPI)

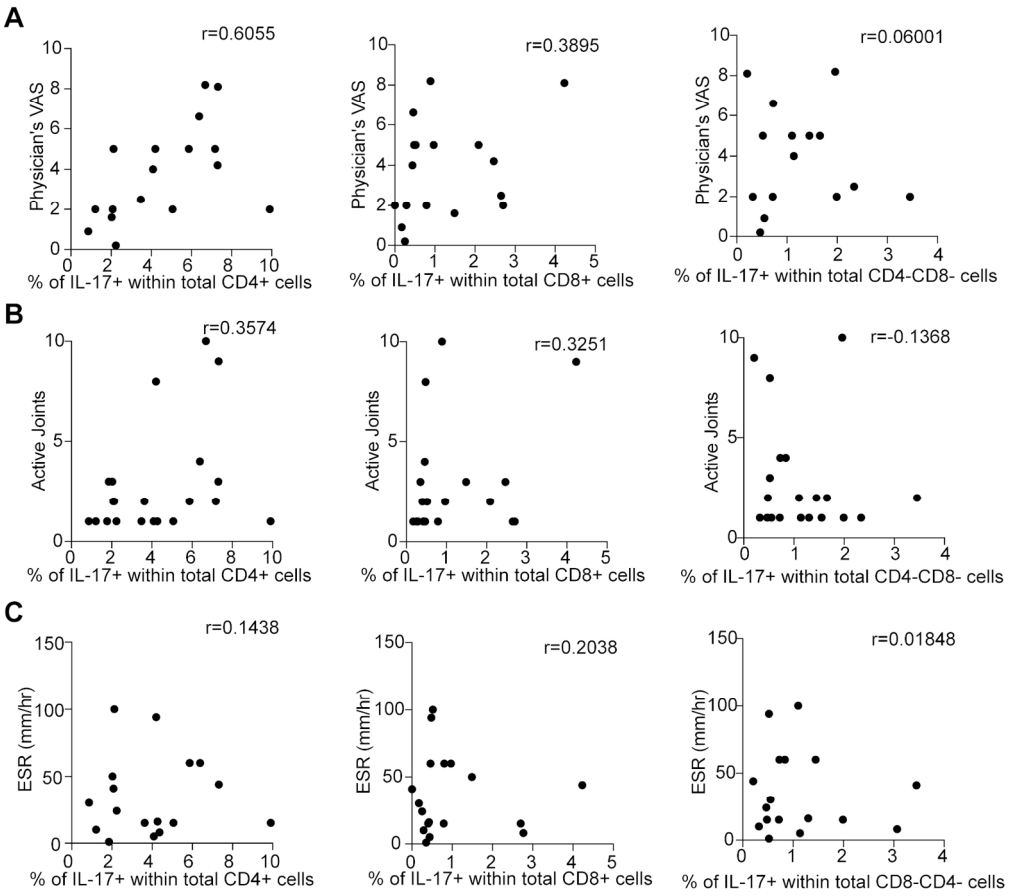

SUPPLEMENTARY FIGURE 2: IL-17A+ T cell subsets can be associated with clinical measure of disease severity. Scatter plots showing relationship between (A) physician's VAS (n=15), (B) active joints (n=21) and (C) ESR (n=17) and the frequency of IL-17+CD4+ T cells, IL-17+CD8+ T cells and IL-17+CD4-CD8- T cells within JIA-SFMC. Statistical analysis carried out by Spearman correlation analysis with Bonferroni's correction for multiple testing.

151x134mm (300 x 300 DPI)

Supplementary Table 1. Patient demographics

	Adult healthy control (n=22)	Child healthy control (n=7)	Oligo-arthritis (n=22)	Polyarticular arthritis (n=14)	Enthesitis related arthritis (n=25)	Psoriatic arthritis (n=10)
No. male/female	8/14	5/2	10/12	6/8	22/3	2/8
Age at sampling (years), median (IQR)	25.99 (24.93-30.19)	6.29 (5.48 – 8.31)	8.70 (7 – 11.17)	10.97 (9.39 – 12.86)	14.00 (12.00 – 16.46)	12.32 (11.20 – 13)
Treatment received within preceding 6 months of sample: MTX (%)	n/a	n/a	9/22 (41%)	11/14 (78.57%)	12/25 (48%)	4/10 (40%)
Treatment received within preceding 6 months of sample: Biological therapy (%)	n/a	n/a	0/22 (0%)	3/14 (21.42%)	1/25 (4%)	2/10 (20%)
No. of swollen/tender joints involved at time of sampling, median (IQR)	n/a	n/a	1 (1 -2)	2 (2 – 3.5)	2 .50 (1 -4.5)	2 (1.25 – 4.25)
ESR mm/hr at time of sampling, median (IQR)	n/a	n/a	25 (11 – 46)	41 (12 – 68)	19 (15 - 60)	30 (12 – 21)
HLA-B27+ (%)	n/a	n/a	n/a	n/a	21/25 (84%)	n/a
RF + (%)	n/a	n/a	n/a	2/14 (14.28%)	n/a	n/a

Supplementary Table 2. List of Antibodies for Flow Cytometry and Cell Sorting

Marker	Fluorochrome	Clone	Supplier
CD1a	PE	H149	eBiosciences
CD3	PE	UCHT1	Biolegend
CD3	V500	UCHT1	BD Biosciences
CD3	BV605	OKT3	BioLegend
CD3	BV711	OKT3	BioLegend
CD4	BV711	OKT4	BioLegend
CD8a	FITC	SK1	BD Biosciences
CD8a	APC	SK1	eBioscience
CD11c	PE	3.9	BioLegend
CD14	PE	61D3	BioLegend
CD16	PE	B73.1	eBiosciences
CD19	PE	HIB19	BioLegend
CD34	PE	561	BioLegend
CD45	BV421	HI30	BioLegend
CD45	PE-CY7	HI30	BioLegend
CD94	PE	DX22	BioLegend
CD123	PE	6H6	BioLegend
CD127	FITC	EBIORDR5	eBiosciences
CD127	BV711	A019D5	BioLegend
CD161	APC	HP-3G10	eBiosciences
CD161	BV605	HP-3G10	BioLegend
CD161	PE-CY7	HP-3G10	eBiosciences
CD161	BV421	HP-3G10	BioLegend
CRTH2	FITC	BM16	BioLegend
cKit	BV421	104D2	BioLegend
BDCA2	BV510	1A4	BioLegend
FcεRIα	PE	AER-37	BioLegend
NKp44	APC	P44-8	BioLegend
αβTCR	PE	IP26	BD Biosciences
γδTCR	PE	B1	BD Biosciences
IL-17AA	BV605	BL168	BioLegend

Supplementary Table 3. List of primer sequences for PCR

Gene	Primer Sequences 5'- 3'		Annealing Temp (°C)
ACTB	F	AGA TGAC CCAGATCATGTTTGAG	60
	R	AGGTCCA GACGCAG GATG	
TBX21	F	CCCCAAG GAATTGAC AGTTG	60
	R	GGGAAAC TAAAGCTC ACAAAC	
IFNG	F	TGACCAG AGCATCCA AAAGA	60
	R	CTCTTCGA CCTCGAAA CAGC	
GATA3	F	ACCACAAC CACACTCT GGAGGA	60
	R	TCGGTTTC TGGTCTG GATGCCT	
IL13	F	A TTGCTCT CACTTGCC TTGG	60
	R	GTCAGGTT GATGCTC CATACC	
RORC	F	AATCTGGA GCTGGCC TTTCA	60
	R	CTGGAAG ATCTGCAG CCTTT	
AHR	F	CTTAGGCT CAGCGTC AGTTA	60
	R	GTAAGTTC AGGCCTT CTCTG	
IL17A	F	AATCTCCA CCGCAAT GAGGA	60
	R	ACGTTCCC ATCAGCGT TGA	
IL22	F	CCCATCA GCTCCCA CTGC	60
	R	GGCACCA CCTCCTG CATATA	

Supplementary Table 4. Uncorrected p values for correlation analyses.

Figure	X Axis	Y Axis	Uncorrected p Value
Fig. 2E	% of ILC1 within total live cells	Physician's VAS	p=0.0179
Fig. 2E	% of NCR-ILC3 within total live cells	Physician's VAS	p=0.0048
Fig. 2E	% of NCR+ILC3 within total live cells	Physician's VAS	p=0.0352
Fig. 2F	% of ILC1 within total live cells	Active Joints	p=0.4552
Fig. 2F	% of NCR-ILC3 within total live cells	Active Joints	p=0.0055
Fig. 2F	% of NCR+ILC3 within total live cells	Active Joints	p=0.8539
Fig. 2G	% of ILC1 within total live cells	ESR (mm/hr)	p=0.2307
Fig. 2G	% of NCR-ILC3 within total live cells	ESR (mm/hr)	p=0.0830
Fig. 2G	% of NCR+ILC3 within total live cells	ESR (mm/hr)	p=0.1599
Fig. 3D	% of IL-17+ within CD4+ T cells	% of NCR-ILC3 within total live cells	p=0.0220
Fig. 3E	% of IL-17+ within CD8+ T cells	% of NCR-ILC3 within total live cells	p=0.0030
Fig. 3F	% of IL-17+ within CD4-CD8- T cells	% of NCR-ILC3 within total live cells	p=0.0893
Sup Fig. 2A	% of IL-17+ within CD4+ T cells	Physician's VAS	p=0.0114
Sup Fig. 2A	% of IL-17+ within CD8+ T cells	Physician's VAS	p=0.1263
Sup Fig. 2A	% of IL-17+ within CD4-CD8- T cells	Physician's VAS	p=0.8320
Sup Fig. 2B	% of IL-17+ within CD4+ T cells	Active Joints	p=0.1117
Sup Fig. 2B	% of IL-17+ within CD8+ T cells	Active Joints	p=0.1620
Sup Fig. 2B	% of IL-17+ within CD4-CD8- T cells	Active Joints	p=0.5651
Sup Fig. 2C	% of IL-17+ within CD4+ T cells	ESR (mm/hr)	p=0.5818
Sup Fig. 2C	% of IL-17+ within CD8+ T cells	ESR (mm/hr)	p=0.4069
Sup Fig. 2C	% of IL-17+ within CD4-CD8- T cells	ESR (mm/hr)	p=0.9448

P values below 0.0023 are considered statistically significant once corrected with Bonferroni's post-test for multiple testing.